MRI-powered biomedical devices

Sierra Hovet[1], **Hongliang Ren**[2], **Sheng Xu**[3], **Bradford Wood**[3], **Junichi Tokuda**[4], and **Zion Tsz Ho Tse**[1]

[1]College of Engineering, University of Georgia, Athens, GA, USA

[2]Department of Biomedical Engineering, National University of Singapore, Singapore

[3]Center for Interventional Oncology, Department of Radiology and Imaging Sciences, National Institutes of Health, Bethesda, MD, USA

[4]Department of Radiology, Brigham and Women's Hospital, Harvard Medical School, Boston, MA, USA

Abstract

Magnetic resonance imaging (MRI) is beneficial for imaging-guided procedures because it provides higher resolution images and better soft tissue contrast than computed tomography (CT), ultrasound, and X-ray. MRI can be used to streamline diagnostics and treatment because it does not require patients to be repositioned between scans of different areas of the body. It is even possible to use MRI to visualize, power, and control medical devices inside the human body to access remote locations and perform minimally invasive procedures. Therefore, MR conditional medical devices have the potential to improve a wide variety of medical procedures; this potential is explored in terms of practical considerations pertaining to clinical applications and the MRI environment. Recent advancements in this field are introduced with a review of clinically relevant research in the areas of interventional tools, endovascular microbots, and closed-loop controlled MRI robots. Challenges related to technology and clinical feasibility are discussed, including MRI based propulsion and control, navigation of medical devices through the human body, clinical adoptability, and regulatory issues. The development of MRI-powered medical devices is an emerging field, but the potential clinical impact of these devices is promising.

Keywords

MRI powered; MRI conditional; mechatronics; microbots

Correspondence: Zion Tsz Ho Tse, College of Engineering, University of Georgia, Driftmier Engineering Center Annex Room 111, 597 D.W. Brooks Dr, Athens, GA, 30602; ziontse@uga.edu.

Introduction

Clinical motivation

Magnetic resonance imaging (MRI) is frequently used for diagnostics over computed tomography (CT), ultrasound, and X-ray because it produces higher resolution images and better soft tissue contrast. MRI also has the ability to scan any 2D cross-section or 3D volume of a body without patient repositioning between scans. Because of this, MRI can be used during medical procedures to help guide instruments through the body. MRI-guided procedures can allow diagnosis, treatment, and post-procedural evaluation to be performed in a single clinical workflow, thereby streamlining the entire process and benefitting both doctors and patients.

MRI and robotics researchers have worked together to design medical devices which perform procedures under MRI guidance (1–3). Robotic systems can assist clinicians with preoperative planning and improve the accuracy, precision, repeatability, and safety of surgical operations. One of the main obstacles to the development of MRI-conditional medical devices is the large set of design constraints imposed by the strong magnetic field and RF environment of MRI scanners. Because all components present in the MRI suite must be able to function in the MR environment without generating mutual interference, feasible materials and actuation principles are limited.

Some interventional devices need to be (or would benefit from being) untethered and remotely operated during an MRI scan, such as gastrointestinal endoscopes. MRI-powered and guided medical devices that can navigate internal spaces of the human body for therapy and diagnoses have the potential to reach areas currently inaccessible by traditional surgery and perform minimally invasive interventions. For these applications, pneumatic or electric actuation may not be feasible. Therefore, a wireless source of power and control that can be operated during an MRI scan is needed. The magnetic coils used for MRI could potentially be used for generating forces in the mechatronic components of MR conditional devices (4). While the magnetic gradients generated by clinical MRI systems can exert only a limited amount of force on actuators, MRI-based propulsion has been demonstrated to be feasible for certain applications (5, 6).

The technologies for MRI-powered/controlled devices for interventional MRI procedures reviewed in this paper are still in their early stages and require further development to reach clinical adoption. Interfacing between MRI scanners and MRI-powered/controlled devices mainly requires software modifications for strategically controlling the radiofrequency used to power and control the devices, which does not require modification of the MRI scanners. Therefore, these technologies could potentially be adopted for clinical use regardless of MRI scanner brands and makes.

MRI-powered medical devices

This section focuses on MRI-powered medical devices, highlighting applications in interventional tools, endovascular microbots, and closed-loop controlled MRI devices. Table 1 summarizes key information about the studies discussed in this section.

Interventional tools

Catheters—Normally, image-guided endovascular procedures use digital subtraction angiography (DSA). However, DSA emits ionizing radiation and its contrast agents exhibit nephrotoxicity. These two issues do not present in MRI. Unlike DSA, MRI can visualize soft tissue and provide information about physiology and metabolism. In 2007, Settecase et al. showed that by winding a wire around the tip of an endovascular catheter to create solenoid coils, an MRI scanner can be used to simultaneously steer (Figure 1a) and visualize the catheter in real time (15). The aim of this study was to derive and experimentally validate an equation relating catheter deflection to: number of solenoid turns, applied current, catheter bending stiffness, the magnetic field of the MRI scanner, the initial angle between the catheter tip orientation and the main magnetic field direction, and the unconstrained catheter length. By successfully explaining the relationship between catheter deflection and physical factors, the study set a solid foundation for further exploration of MRI-guided endovascular procedures and catheter design.

The catheter design proposed in (15) achieved MRI-assisted remote steering and visualization, but did not take into account resistive heating in the solenoid coils. Therefore, Bernhardt et al. in 2011 further developed the design by exploring a solution to resistive heating in the coils. The new design (Figure 1b) utilized a lithographic technique called Laser Lathe to fabricate solenoid coils around an alumina tube (16). Raychem shrink tubing is used to insulate the body from heat in the coils, and saline coolant flows inside the tube to remove heat from the coils. Alumina was chosen because it facilitates heat transfer. *In vitro* and *in vivo* testing demonstrated promising results—even when using worst case scenario conditions—so Bernhardt et al. predicted their design would prove safe for both clinical operation and failure conditions in future studies.

Gauss gun for localized therapies—MRI can be used to navigate and propel millimeter-scale robots (millirobots) through the fluid-filled cavities of the human body. However, MRI is not capable of propelling a robot with enough force to puncture tissue. The ability to puncture tissue is a desirable feature for MRI-powered millirobots because it would allow for various localized therapies such as releasing trapped fluid from a membrane, opening a blocked passageway, or delivering drugs to tissue. Becker et al. (2015) designed multiple components to a Gauss gun (Figure 1c) that can be individually moved through fluid-filled cavities, assembled at the therapy site, fired so that a needle penetrates tissue, disassembled, and navigated back out of the body. Each component of the Gauss gun has a VeroWhite polymer shell—printed with a Stratasys Objet printer—containing magnetic chrome steel spheres and nonmagnetic metal spacers (that are standard parts). The projectile is a standard needle tip welded to a small chrome steel sphere. This study shows that it is possible to overcome the inability of MRI to directly power a projectile for puncturing tissue, but further optimization for clinical use is required, as well as a closed-loop control system (17).

Biopsy needle—In 2011, Vartholomeos et al. published their novel design of a robotic actuator for needle biopsy that could be powered and controlled by an MRI scanner without affecting image SNR at the region of interest (18). The design was simple compared to many

existing actuators at the time which required motors, wires, complicated installation, and could have negative effects on bandwidth and imaging SNR. The actuator design called for the actuator to be constructed from nonferrous materials; the only ferrous component was to be enclosed within a cavity inside a rotor so that rotation could be achieved by generating a force on the ferrous component with the application of magnetic field gradients. The prototyped actuator (Figure 1d)—made of Legos, a ferromagnetic sphere, and a non-ferromagnetic biopsy needle—generated enough force to puncture epicardial tissue when operated with a clinical 1.5 T MRI scanner (18).

Vartholomeos et al. (2012) improved their design for an MRI-powered actuator described in (18) by interleaving actuation and imaging to achieve closed-loop position control of the biopsy needle displacement. Tracking the needle position was made possible by attaching a passive fiducial marker to the rack holding the needle (Figure 1d). Needle position control was limited to one degree of freedom, but Vartholomeos et al. stated their intention to expand control to multiple degrees of freedom in future work (19).

Endovascular microbots

Magnetohydrodynamic swimming robot—Magnetohydrodynamic (MHD) voltages induced in the magnetic field of an MRI scanner can be used to propel endocapsules inside the human body while MRI is used to visualize the endocapsules. In 2015, Gregory et al. prototyped an endocapsule (Figure 2a) which moved in response to changes in input power, with a peak force of 0.31 mN (20). These results demonstrated that an MHD-driven endocapsule is feasible in an MRI environment. These devices could be capable of moving through the bloodstream to deliver treatments or assist with surgeries.

Microbot control method—In 2009, Arcese et al. modeled a device experiencing both magnetic and hydrodynamic forces as a nonlinear control system; the device represents a microbot inside an MRI scanner. The aim of the study was to define a method of moving the device along a specific desired path. Arcese et al. developed a control method to be used along with a high gain observer, and simulations indicated promising results (21).

Microbot flagellar propulsion—Behkam and Sitti (2005) created a swimming microbot inspired by the peritrichous flagellation method of propulsion used by bacteria (22). The prototype (Figure 2b) included a two-phase stepper motor, Styrofoam jacket, and steel wire "flagellum." The microbot was MRI-conditional and designed to swim in low velocity biofluids so it could be used for medical interventions in inaccessible areas such as the eyeball cavity, cerebrospinal fluid, and the urinary system.

Coil-based swimming mechanism—In 2008, Kósa et al. designed a capsule which could be useful for untethered navigation through the small intestine for disease diagnoses (23). The design (Figure 2c) included three coils enclosed in a capsule; the magnetic field of the MRI induces current in the coils, which flows into nine other coils (three coils along each of three swimming tails). The current in the coils on the swimming tails interacts with the MRI's magnetic field and produces a waving motion. Experiments showed that a 10 mm long tail could produce a velocity of 7.9 mm/s in a 3T static magnetic field.

In 2012, Kósa et al. presented another swimming robot design similar in concept but different in shape (Figure 2d) (24). The application for the new design was suggested to be stomach and bowel inspection, and the device is meant to be swallowed by the patient. The design is rather large for this application (the capsule is ϕ12mm $\times$ 32mm not including the swimming tails) and the researchers stated the design does not scale down well. Powering, propelling, and visualizing the device with MRI shows promise, however.

MRI steering coils—Mathieu et al. (2007) presented a method to integrate steering coils into an MRI system to improve microbot steering. The study used MRI steering coils to steer magnetite Fe_3O_4 microparticles through a Y-shaped microchannel (based on human vasculature but with a mean fluid velocity ten times as fast as arterioles of the same diameter) between a Maxwell pair in an MRI bore. Experimental results were used to estimate the strength of the magnetic gradient the steering coils would need to produce for clinical applications. In addition, the experiment resulted in proof of concept of microparticle steering using magnetic gradients during MRI for applications related to the human cardiovascular system (25). Overall, the results showed promise, and future improvements could lead to the widespread use of microbots for many medical applications.

Closed-loop controlled MRI robots

Actuation for general needle insertion—As mentioned previously, Vartholomeos et al. designed a needle positioning and driving system (Figure 1d) which is both powered and controlled by an MRI scanner (18, 19). In 2013, Vartholomeos et al. presented guidelines for further developing and implementing the technology described in (18) and (19). They also provided analytical (Figure 3) and experimental (Figure 4) information about the closed-loop control method described in (19). Imaging pulse sequences (used to estimate the position of the needle) are interleaved with propulsion pulse sequences (used to actuate needle movement) to achieve closed-loop control of needle movement. Vartholomeos et al. also demonstrated that open-loop control of slip angle has the potential to be successfully integrated into the design. The study specified actuator design parameters for achieving desired needle insertion force, since the force requirement varies depending on needle size and design, and tissue type. Further research will focus on identifying actuator materials with low tolerances, low friction, but still low enough cost to allow for single-use actuators. Actuating additional degrees of freedom is also a key area for improvement (26).

Actuation of system designed for breast therapy—In 2014, Ouchi et al. developed an actuator (Figure 5a) that is powered and controlled by an MRI scanner (27). The actuation principle relies on the interaction of magnetic forces generated by the scanner and a ferromagnetic particle embedded in the actuator. The ferromagnetic particle is located in a rotor to convert magnetic energy into mechanical energy. Control of multiaxial movement is achieved using a common imaging sequence called turbo spin echo (TSE). Future studies will address the need for increased torque by improving the mechanism, possibly by adjusting the gear ratio. A clear understanding between the imaging sequence and the movement of the actuator is also required before the system can be applied to procedures including needle biopsies and esthesiometry. A major goal of the research is to automate such procedures.

In 2015, Ouchi et al. incorporated their previous MRI-powered actuator design (27) into a new robotic system (Figure 5b) capable of positioning a needle perpendicular to any point on half of a spherical surface (28). This needle positioning system is important because the MRI gantry is too small for manual needle positioning, meaning patients have to be moved in and out of the scanner for traditional MRI-assisted procedures. Remote needle positioning would decrease procedure time and reduce errors caused by patient movements while being wheeled in and out of the scanner. The system is especially suited to assisting cryoablation of breast cancer, but future studies are needed to explore the effects of the ferromagnetic sphere on MR images, and to enable the system to manipulate a needle and needle guide.

Technical challenges and future directions

MRI-based magnetic propulsion and control

MRI-conditional technologies for actuation, position sensing, and force sensing have been developed, some of which use the electromagnetic coils of the MRI scanner as a power source. The entire system is greatly simplified when both the imaging and robotic components are powered by the same source. This is an advantage because MRI-conditional robot designs typically require either image quality or design simplicity to be sacrificed.

The electromagnetic coils of an MRI scanner create a magnetic field, which exerts force on ferromagnetic objects. This is the actuation principle of MRI-based propulsion, which was proposed in (5) and demonstrated in a clinical MRI. The force, $F_{magnetic}$, exerted by the MRI magnetic field gradients is

$$\vec{F}_{magnetic} = RV_{ferro}\left(\vec{M} \cdot \nabla\right)\vec{B}$$

where R is the duty cycle representing the amount of time for which the magnetic gradients are applied relative to the length of each cycle, V_{ferro} is the volume of the ferromagnetic body (m^3), M is the magnetization of the material (A/m), B is the magnetic field (T), and $(\vec{M} \cdot \nabla)\vec{B}$ is the directional derivative of the magnetic field. One drawback of MRI-based propulsion is that the magnetic field can only be used to power one function at a time, either imaging or propulsion. The magnetic field generation must be programmed as a sequence that switches between taking an image and delivering a propulsion force. Image quality requirements and propulsion duty cycle requirements affect the feasible repetition rate of the imaging/propulsion process. A repetition rate of several executions per second is attainable with quick imaging sequences. However, in order to increase the repetition rate beyond several executions per second, the number of k-space line acquisitions in the imaging sequences would need to be reduced, leading to lower spatial resolution in the image. A 20–30 Hz repetition rate has been demonstrated, and could possibly be used to propel and control microbots (29).

Navigation through vasculature

Small robots can be used to access any part of the human body for therapeutic purposes by navigating through vasculature. Using an MRI scanner to visualize the robots is reasonable

because MRI is common in hospitals and provides excellent imaging of the cardiovascular system. However, the robots and actuation methods have many design constraints because they must be MRI-conditional. In order to fulfill the size and actuation requirements for this application, one possibility is to assemble many magnetic nanoparticles into one microbot. The nanoparticles could be bound with a biodegradable ligand or designed to self-assemble through local magnetic or surfacic forces (30). For certain applications it may be helpful for the microbot to be able to disintegrate, such as to assist with drug release.

The vessel radius and blood flow velocity of different areas of vasculature in the body must be taken into consideration when designing a microbot for cardiovascular navigation. For example, large vessels with high blood flow might require the robots to use a propelling force to resist drag. The actuation force attainable with MRI-based propulsion is relatively low in comparison to drag forces in the cardiovascular system, but a sufficient quantity of ferromagnetic material and strong attractive forces between nanoparticles are likely to enable steering. In small vessels with low blood flow, the robot may need either mechanisms or physical characteristics which help to avoid embolism or thrombosis. Figure 6 shows the radius and blood flow velocities in different types of blood vessels.

One safety concern about controlling microbots in the vasculature is the possibility of the microbots increasing the risk of embolization, which could be addressed by coating the robots with materials that prevent blood clots (31–35). Another safety concern is magnetic hazards; time-varying magnetic fields can have neurological effects, so the FDA has regulations on the standard slew rates of time-varying magnetic gradients in clinical MRI scanners.

Clinical regulatory issues and practical considerations

Clinical regulatory agencies such as the U.S. Food and Drug Administration (FDA) and European Medicines Agency (EMA) evaluate medical devices and determine whether they can be applied clinically. When designing MR conditional medical devices, it is important to ensure that designs comply with the regulations specified by these agencies. Regulations are focused on reliability, ease of use, and user safety. MR conditional medical devices will carry some risk (like any medical device or procedure) but the probable benefits to patients have to outweigh the probable risks (7). The risk-to-benefit ratio of the proposed device will be compared to current technology with the same application to assess clinical adoptability. The implementation costs—in terms of time, effort, and money—are also factors in clinical adoption.

MR conditional devices have the potential to perform minimally invasive medical procedures with improved flexibility, dexterity, safety, and accuracy in comparison to existing methods. Some of the most important characteristics for clinical applications are ease of use, high repeatability, time effectiveness, and cost effectiveness. A short learning curve for clinicians is advantageous, as it reduces training time and implementation cost. Shortening procedure times is extremely important, as it benefits the patient, frees up clinicians' time, and reduces costs. Clinicians' input should be used when developing design requirements and specifications related to both function and operation so the final product is tailored to the end users' needs and the clinical environment.

Conclusion

The results of the research papers reviewed above indicate that optimism towards the future of MR conditional robotics is reasonable. Standardized tests for MRI compatibility designations (i.e. MR safe and MR conditional) provide a framework for designing mechatronic components and choosing materials, and regulatory agencies are equipped to approve MR conditional devices for clinical use. The foundation for clinically relevant research is laid, so partnering with clinicians to focus research on specific medical applications is an excellent way to ensure that academic pursuits align with goals for improving medical procedures.

Acknowledgments

References

1. Chen Y, Zion TT, Wang W, et al. Intra-cardiac MR imaging & MR-tracking catheter for improved MR-guided EP. J Cardiovasc Magn Reson. 2015; 17:1–2. [PubMed: 25589308]

2. Hempel E, Fischer H, Gumb L, et al. An MRI-compatible surgical robot for precise radiological interventions. Comput Aided Surg. 2003; 8:180–91. [PubMed: 15360099]

3. Wang W, Viswanathan AN, Damato AL, et al. Evaluation of an active magnetic resonance tracking system for interstitial brachytherapy. Medical physics. 2015; 42:7114–21. [PubMed: 26632065]

4. Vartholomeos, P; Aylak, SS; Mavroidis, C, editors. Computational Studies of Controlled Nanoparticle Agglomerations for MRI-Guided Nanorobotic Drug-Delivery Systems; ASME 2010 Dynamic Systems and Control Conference; 2010; American Society of Mechanical Engineers.

5. Mathieu J-B, Beaudoin G, Martel S. Method of propulsion of a ferromagnetic core in the cardiovascular system through magnetic gradients generated by an MRI system. IEEE Transactions on Biomedical Engineering. 2006; 53:292–9. [PubMed: 16485758]

6. Pouponneau P, Leroux J-C, Soulez G, et al. Co-encapsulation of magnetic nanoparticles and doxorubicin into biodegradable microcarriers for deep tissue targeting by vascular MRI navigation. Biomaterials. 2011; 32:3481–6. [PubMed: 21315445]

7. ASTM. Standard Practice for Marking Medical Devices and Other Items for Safety in the Magnetic Resonance Environment. F2503-13 West Conshohocken, PA: ASTM International; 2013. [Available from: www.astm.org

8. ASTM. Standard Test Method for Measurement of Magnetically Induced Displacement Force on Medical Devices in the Magnetic Resonance Environment. F2052-06e1 West Conshohocken, PA: ASTM International; 2006. [Available from: www.astm.org

9. ASTM. Standard Test Method for Measurement of Magnetically Induced Torque on Medical Devices in the Magnetic Resonance Environment. F2213-06 West Conshohocken, PA: ASTM International; 2011. [Available from: www.astm.org

10. ASTM. Standard Test Method for Evaluation of MR Image Artifacts from Passive Implants. F2119-07 West Conshohocken, PA: ASTM International; 2013. [Available from: www.astm.org.

11. Chinzei, K, Kikinis, R, Jolesz, F, editors. MR Compatibility of Mechatronic Devices: Design Criteria 2nd International Conference on Medical Image Computing and Computer-assisted Interventions. Cambridge, UK: 1999.

12. Schenck JF. The role of magnetic susceptibility in magnetic resonance imaging: MRI magnetic compatibility of the rst and second kinds. Medical Physics. 1996; 23:815–50. [PubMed: 8798169]

13. Shellock FG. Magnetic resonance safety update 2002: Implants and devices. J Magn Reson Imaging. 2002; 16:485–96. [PubMed: 12412025]

14. ASTM. Standard Test Method for Measurement of Radio Frequency Induced Heating Near Passive Implants During Magnetic Resonance Imaging. F2182-02a West Conshohocken, PA: ASTM International; 2002. [Available from: www.astm.org

15. Settecase F, Sussman MS, Wilson MW, et al. Magnetically-assisted remote control (MARC) steering of endovascular catheters for interventional MRI: a model for deflection and design implications. Medical physics. 2007; 34:3135–42. [PubMed: 17879774]

16. Bernhardt A, Wilson MW, Settecase F, et al. Steerable catheter microcoils for interventional MRI: reducing resistive heating. Academic radiology. 2011; 18:270–6. [PubMed: 21075017]

17. Becker, AT; Felfoul, O; Dupont, PE, editors. Robotics and Automation (ICRA), 2015 IEEE International Conference on. IEEE; 2015. Toward tissue penetration by MRI-powered millirobots using a self-assembled Gauss gun.

18. Vartholomeos, P; Qin, L; Dupont, PE, editors. 2011 IEEE/RSJ International Conference on. IEEE; 2011. MRI-powered actuators for robotic interventions. Intelligent Robots and Systems (IROS).

19. Vartholomeos, P; Bergeles, C; Qin, L; Dupont, PE, editors. The Hamlyn Symposium on Medical Robotics. 2012. Closed-loop position control of an MRI-powered biopsy robot.

20. Gregory TS, Wu KJ, Yu J, et al. Magnetohydrodynamic-Driven Design of Microscopic Endocapsules in MRI. Mechatronics, IEEE/ASME Transactions on. 2015; 20:2691–8.

21. Arcese, L; Fruchard, M; Ferreira, A, editors. Intelligent Robots and Systems, 2009 IROS 2009 IEEE/RSJ International Conference on. IEEE; 2009. Nonlinear modeling and robust controller-observer for a magnetic microrobot in a fluidic environment using MRI gradients.

22. Behkam, B; Sitti, M, editors. Modeling and testing of a biomimetic flagellar propulsion method for microscale biomedical swimming robots. IEEE Advanced Intelligent Mechanotronics Conference; Monterey, CA. Jul; Citeseer; 2005.

23. Kósa, G; Jakab, P; Jólesz, F; Hata, N, editors. Robotics and Automation, 2008 ICRA 2008 IEEE International Conference on. IEEE; 2008. Swimming capsule endoscope using static and RF magnetic field of MRI for propulsion.

24. Kósa G, Jakab P, Székely G, Hata N. MRI driven magnetic microswimmers. Biomedical microdevices. 2012; 14:165–78. [PubMed: 22037673]

25. Mathieu J-B, Martel S. Magnetic microparticle steering within the constraints of an MRI system: proof of concept of a novel targeting approach. Biomedical microdevices. 2007; 9:801–8. [PubMed: 17566862]

26. Vartholomeos P, Bergeles C, Qin L, et al. An MRI-powered controlled actuator technology for tetherless robotic interventions. Int J Robotics Res. 2013; 32:1536–52.

27. Ouchi, R; Saotome, K; Matsushita, A. , et al., editors. Engineering in Medicine and Biology Society (EMBC), 2014 36th Annual International Conference of the IEEE. IEEE; 2014. Development of MRI-powered modular robotic system.

28. Ouchi, R; Saotome, K; Matsushita, A. , et al., editors. Engineering in Medicine and Biology Society (EMBC), 2015 37t h Annual International Conference of the IEEE. IEEE; 2015. Development of an MRI-powered robotic system for cryoablation.

29. Felfoul O, Mathieu J-B, Beaudoin G, et al. In vivo MR-tracking based on magnetic signature selective excitation. IEEE Trans Med Imaging. 2008; 27:28–35. [PubMed: 18270059]

30. Vartholomeos P, Mayroidis C. Simulation platform for self-assembly structures in mribased nanorobotic drug delivery systems. IEEE international conference on robotics and automation. 2010:5594–600.

31. MacCallum N, Howell C, Kim P, et al. Liquid-Infused Silicone as a Biofouling-Free Medical Material. ACS Biomaterials Science & Engineering. 2015; 1:43–51.

32. Yao X, Hu Y, Grinthal A, et al. Adaptive fluid-infused porous films with tunable transparency and wettability. Nat Mater. 2013; 12:529–34. [PubMed: 23563739]

33. Wong T-S, Kang SH, Tang SKY, et al. Bioinspired Self-Repairing Slippery Surfaces with Pressure-stable Omniphobicity. Nature. 2011; 477:443–7. [PubMed: 21938066]

34. Schmidt-Nielsen, K. Scaling: why is animal size so important?. Cambridge, MA: Cambridge University Press; 1984.

35. Plowman, S, Smith, D. Exercise Physiology. Needham Heights, MA: Allyn and Bacon; 1997.

Key terms

Medical devices used inside an MRI scanner must fulfill a set of criteria related to the MR environment, and safety of clinicians and patients. The following terms defined by the American Society for Testing and Materials (ASTM) are relevant to the design of equipment and robotics for MRI-guided procedures:

- **5 gauss line.** The 5 gauss line surrounds the area around the MR scanner that has a static magnetic field with magnetic induction of < 5 gauss (1 tesla is equal to 10,000 gauss) [8].

- **MR environment.** The term MR environment refers to the magnetic characteristics—consisting of three electromagnetic (EM) fields: the static magnetic field, switched gradient fields, and radio frequency (RF) fields—of the area inside the 5 gauss line (7).

- **MR safe.** A device described as MR safe does not pose any known safety hazards in any MR environment. This term applies to objects that are nonconducting, nonmetallic, and nonmagnetic (7).

- **MR conditional.** A device described as MR conditional does not pose any known safety hazards in a specified MR environment under specified conditions (e.g. static magnetic field strength, radio frequency fields, and specific absorption rate) (7).

Electromagnetic interference with MRI

MRI scanners use a strong magnetic field, switched gradients, and RF fields. The challenges imposed on the development of MR conditional medical devices—including those discussed in this manuscript—can be classified into the following categories:

- Magnetically induced elevated forces and torques

- Image artefacts (image voids) and geometric distortion

- Signal-to-noise ratio (SNR) reduction

- Magnetically induced thermal effect

- Limited workspace for using devices inside the scanner bore

Testing procedures for the first four categories have been detailed and/or standardized by the ASTM International, providing an established method for quantifying the functionality and safety of entire devices or individual components in an MR scanner. The tests are as follows:

- The tests for magnetically induced force (8) and torque (9) are designed to determine the maximum amount of attractive force and torque that would be applied to the test subject (medical device or component) in the MR environment, and to determine if changes are necessary to counteract the magnetic attraction.

- The artifact generation test is used to measure the size of an artifact and evaluate the minimum separation distance between the imaging volume and test subject that will not affect image quality. The image geometrical distortion test is used to determine whether the placement of the test subject at the distance suggested by the artifact generation test is suitable by assessing if the test subject causes a warping effect in the image (10).

- The SNR reduction test is used to show how the EM interference from the test subject affects image quality. The result demonstrates the image quality degradation that might occur if several of the tested components were used in the robot design (11–13).

- The thermal effect test is used to quantify temperature fluctuations of the test subject caused by the RF pulses and switched gradient magnetic fields generated by the MRI scanner. This test is important for ensuring that dangerously high voltages are not induced, since this could result in sparking, skin burns, and fire (14).

When choosing materials for an MR conditional device, the structural components of the device should be made of materials with low magnetic susceptibility. Ideally, actuators and sensors should be MR conditional as well. The above tests can be used to quantitatively evaluate alternatives for each component of a device. Even if each

component tests well, the assembled device may not be MR conditional, so the entire prototype must also be tested for functionality and safety in the MR scanner.
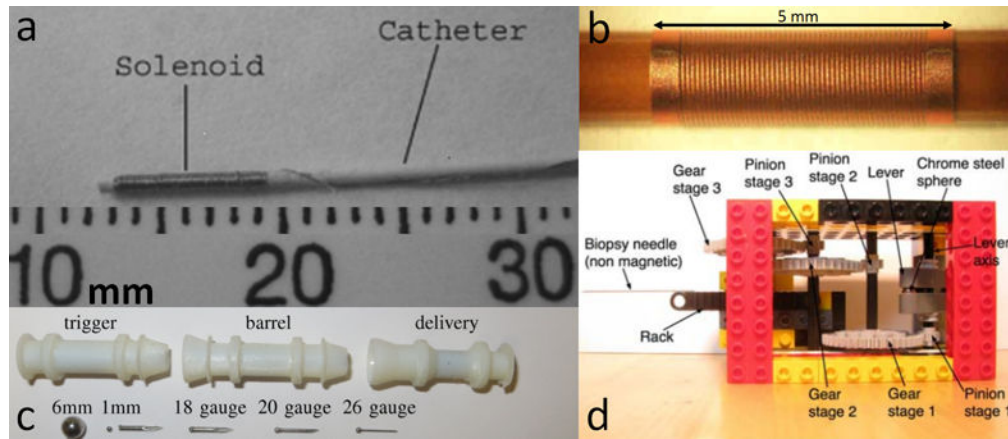
Figure 1.
(a) 1.8 F catheter with 100 turn solenoid made of magnet wire wrapped around the tip (15);
(b) solenoid coil fabricated onto a tube using Laser Lathe (16); (c) components of Gauss gun
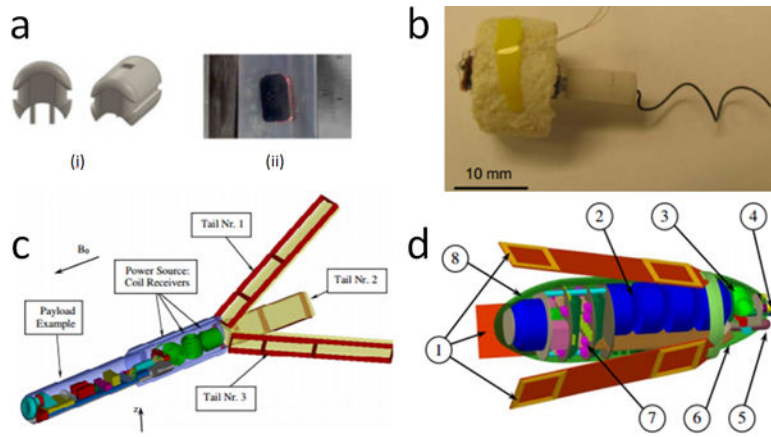(17); (d) 10 cm × 6 cm × 6 cm actuator with attached biopsy needle (18).

Figure 2.
(a) MHD swimming robot endocapsule (i) design and (ii) prototype (20); (b) swimming microbot prototype (22); (c) swimming robot design by Kósa et al. in 2008 (23); (d) swimming robot design by Kósa et al. in 2012 (24).
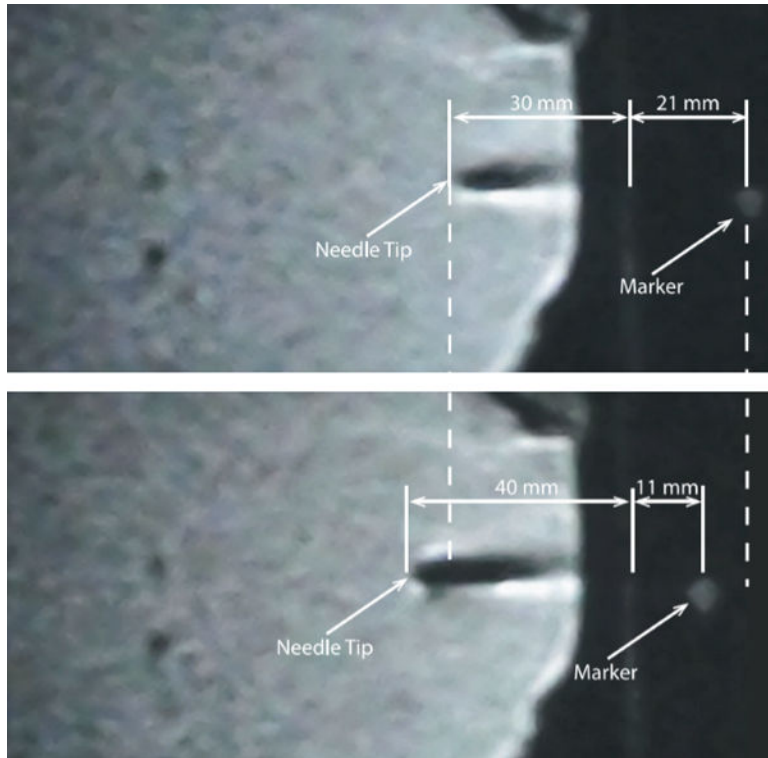
Figure 3.
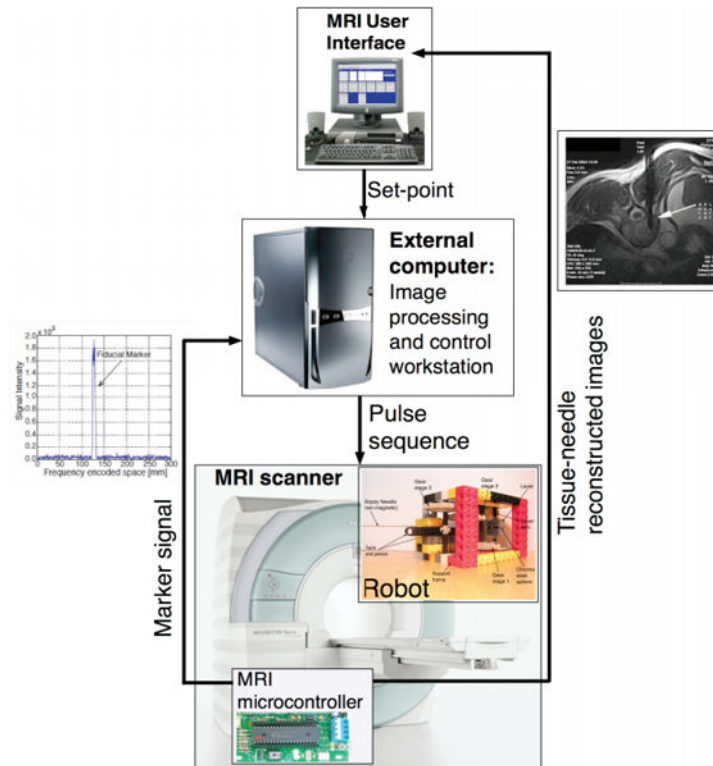Closed loop architecture of the MRI-powered robot (19, 26).

Figure 4.
MR images of position-controlled needle displacement into chicken breast: before (top) and after (bottom) completion of the motion (19, 26).
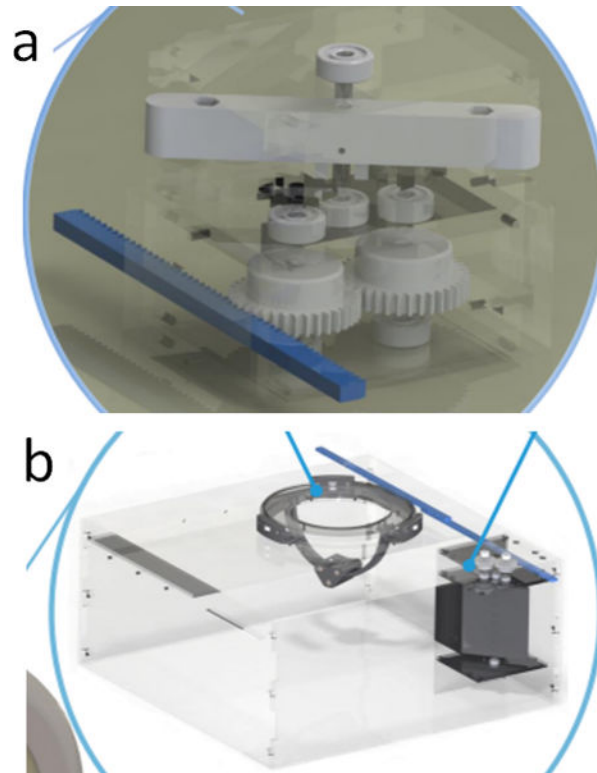
Figure 5.
(a) Actuator prototype (dimensions: 80 mm × 55 mm × 70 mm) (27); (b) actuator and needle positioning mechanism (dimensions: 80 mm × 55 mm × 70 mm) (28).
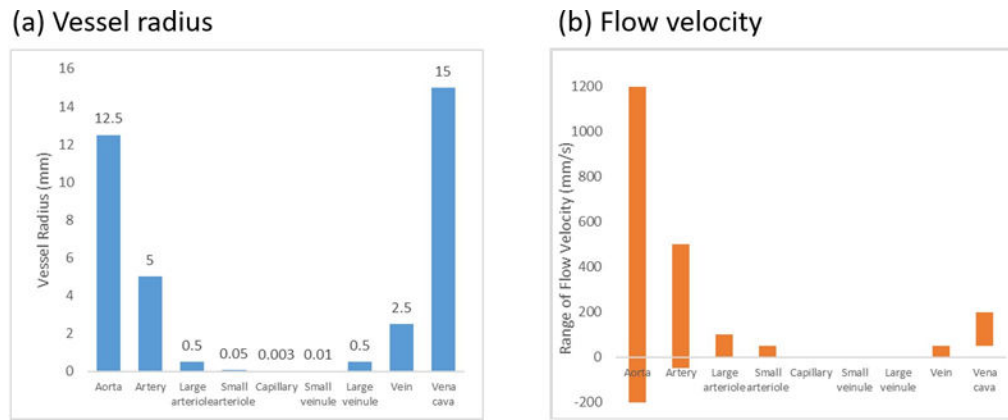
Figure 6.
(a) Vessel radius and (b) average flow velocity versus different types of blood vessels. Negative values of the flow velocity in (b) stand for the flow back values in arterial vessels (34, 35).

Table 1

Technical details from studies on MRI-powered biomedical devices.

Application	Technical Significance	Size/Volume	Actuation Control Principle	Manufacturability	Lead Author/Year/Ref	Institute
Remote steerage of endovascular catheter under MRI-guidance	MRI is safer and has more capabilities (including soft tissue visualization) than digital subtraction angiography (DSA) normally used for endovascular procedures.	Wire solenoid coils increased catheter diameter by 0.45 to 0.6 F (F = 1/3 mm). Solenoid coils were between 3 and 10 mm long depending on number of turns.	Applying current to a solenoid coil wrapped around the tip of a catheter in a magnetic field causes the catheter tip to deflect. The induced magnetic moment causes local field inhomogeneity which allows for MRI visualization.	44 AWG magnet wire was wound around the tip of a catheter to create 50–150 solenoid turns. The loose ends of the wire were braided and wrapped around the length of the catheter.	Settecase, F. 2007 [16]	University of Toronto, Ontario, Canada; University of California, San Francisco; University of Pennsylvania; Children's Hospital of Philadelphia.
Investigate resistive heating in microwires used for MRI-assisted remote catheter steering and present a possible solution	*In vitro* results showed an acceptable effluent temperature increase, and *in vivo* results showed no thermal injury to vessel walls, so the alumina tube is very promising for future studies.	-	The solenoid coils can be cooled with saline coolant flowing inside the lumen of a catheter tip made of materials that facilitate heat transfer.	Solenoid coils fabricated onto alumina tube with lithographic method called Laser Lathe. Raychem shrink tubing added to shield body from coils. Customized alumina tube added to distal end of catheter.	Bernhardt, A. 2011 [17]	Lawrence Livermore Research Laboratory, CA; University of California, San Francisco; University of Pennsylvania; Children's Hospital of Philadelphia; University of Toronto, Ontario, Canada.
Internal tissue penetration by millirobots for localized therapies	Gauss gun allows the millirobots to apply more force to tissue than when just using MRI gradients	3 roughly cylindrical components to the Guass gun, each ~40mm long with ~12mm diameter	MRI control to assemble and fire Gauss gun	Gauss gun shells can be printed with Stratasys Objet printer and other components are standard	Becker, Aaron T. 2015 [18]	University of Houston; Boston Children's Hospital; Harvard Medical School
Robotic assistance for MRI-guided needle biopsy	Actuator powered and controlled by MRI	10 cm × 6 cm × 6 cm	MRI control (sinusoidal cycle of magnetic gradients) to generate force on ferrous component in rotor. 1.2 N generated.	Simple components, some parts standard	Vartholomeos, Panagiotis 2011 [19]	Boston Children's hospital; Brigham and Women's Hospital; Harvard Medical School
Closed-loop position control of actuator described in [19]	Greater control over MRI - guided needle biopsy	-	Imaging (position tracking): gradient echo pulse sequence; Actuation (displacing needle): sinusoidal cycle of magnetic gradients. 1.2 N generated.	External computer and microcontroller required	Vartholomeos, Panagiotis 2012 [20]	Boston Children's Hospital; Dana Farber Cancer Institute; Harvard Medical School
Vascular interventions in areas inaccessible by traditional surgery	Simultaneous propulsion and imaging within MRI scanner	Diameter between 10^{-3} and 1 mm	Magnetohydrodynamic effect used to propel endocapsule. 0.31 mN generated.	Design includes inductive coil, rectifying circuit, electrode plates, and casing.	Gregory, T.S. 2015 [21]	University of Georgia; Tsinghua University, China

Application	Technical Significance	Size/Volume	Actuation Control Principle	Manufacturability	Lead Author/Year/Ref	Institute
Vascular interventions in areas inaccessible by traditional surgery	Nonlinear modeling and robust controller-observer for microbots	Diameter = 600 μm	Magnetic gradients of MR scanner used to propel microbots	-	Arcèse, Laurent 2009 [22]	Institute PRISME, France
Medical interventions in areas inaccessible by traditional surgery	Propulsion method for microbots swimming in low velocity biofluids (e.g. eyeball cavity, cerebrospinal fluid, urinary system)	Diameter=16 mm Length = 46 mm	Two-phase stepper motor powers flagellar motion to propel robot	Motor, Styrofoam jacket, and wire "flagellum" assembled to create prototype	Behkam, B. 2005 [23]	Carnegie Mellon University, PA
Swimming robot for diagnosing diseases in the small intestine	MRI's magnetic fields used for propulsion and wireless energy transfer	Swimming tail: Length: 10 mm Width: 5 mm Thickness: 0.15 mm	MRI magnetic field used to create waving motion in a swimming tail with three coils along its length. 5.5 mN magnetic bending force achieved in each tail.	Capsule contains payload and power source, and is propelled with three swimming tails	Kósa, G. 2008 [24]	ETH Zurich, Switzerland; Brigham and Women's Hospital and Harvard Medical School, Boston
Stomach and bowel inspection	MRI's magnetic fields used for propulsion and wireless energy transfer	Capsule: φ12mm × 32mm Swimming tails: Length: 20mm Width: 5mm	MRI magnetic field used to create waving motion in a swimming tail with two coils along its length. Each tail generates 0.21 mN propulsive force in water.	Capsule contains payload and power source, and is propelled with three swimming tails	Kósa, G. 2012 [25]	Tel Aviv University, Israel; Brigham and Women's Hospital and Harvard Medical School, Boston; ETH Zurich, Switzerland.
Magnetic microparticle steering method	MRI-powered and guided medical microbots could be more feasible with MRI improvements	-	Improving magnetic resonance imaging systems by implementing steering gradient coils in addition to standard imaging coils	Steering coils simple to manufacture and integrate into existing MRI scanners	Mathieu, J.B. 2007 [26]	École Polytechnique de Montréal, Canada
Robotic assistance for MRI-guided needle biopsies requiring different forces	Customizable for different force requirements	10 cm × 10 cm × 6 cm	Imaging (position tracking): gradient echo pulse sequence; Actuation (displacing needle): sinusoidal cycle of magnetic gradients. Force generated in design 1: 0.5 N. Force generated in design 2: 20 N.	Simple components, some parts standard	Vartholomeos, Panagiotis 2013 [27]	Boston Children's Hospital; Dana Farber Cancer Institute; Harvard Medical School
Robotic assistance for MRI-guided procedures (esp. needle biopsy and esthesiometry)	An existing MRI imaging sequence, turbo spin echo (TSE), is used to control multiaxial motion of the robot	Actuator: 80 mm × 55 mm × 70 mm	MRI magnetic field interacts with ferromagnetic particles in robot to actuate device	Simple components and design	Ouchi, R. 2014 [28]	University of Tsukuba, Japan
Robotic assistance for MRI-guided procedures (esp. cryoablation of breast cancer)	Actuator can position a needle perpendicular to any point on the surface of a half-sphere	Actuator: 80 mm × 55 mm × 70 mm	MRI magnetic field interacts with ferromagnetic particles in robot to actuate device. 1.4 N of force needed.	Simple components and design	Ouchi, R. 2015 [29]	University of Tsukuba, Japan